KINETIC MODELLING FOR THERMAL DECOMPOSITION OF THE ALUMINUM HYDROXIDE DRIED, MILLED AND CLASSIFIED

Raluca ISOPESCU[1]*, Gheorghe DOBRA[2], Sorin ILIEV[2], Lucian COTET[2], Alina BOIANGIU[2], Laurentiu FILIPESCU[1]

The paper presents a kinetic study based on Avrami semiempirical model for the thermal decomposition of the aluminum hydroxide in the range 100-400℃. From experimental evidence concerning TG and DSC measurements, different pathways for the solid phase transformations of the gibbsite during heating were assumed for samples with specific particle size ranges. The modelling results stand for the existence of two distinct mechanisms that overlap. The formation of intermediate metastable phases is more likely to take place in samples with large particle sizes, while small particles undergo a rapid and straightforward transformation.

Keywords: gibbsite, thermal transformation, DSC, kinetic modelling

1. Introduction

Gibbsite is an intermediate product in alumina Bayer process and a valuable raw material for manufacture of all the hydrated and non-hydrated products, emerging as transitory phases during multiple ways of gibbsite calcination up to the α-Al_2O_3. Gibbsite and boehmite are the only phases capable to promote as precursors the crystallization of all other transitional phases. Many products from the family $Al(OH)_3$-$3H_2O$ – AlO(OH) - α-Al_2O_3 have important industrial uses as low temperature calcined aluminas and as high temperature ceramic oxides, porous ceramics and castable ceramics. Each category of the above industrial materials has its own standards of quality and special requirements concerning the specific surface, variable particle size distribution, pore size and pore size distribution and the degree of crystallinity [1-4]. Most of the low temperature calcined aluminas are used as**:** adsorbents and water purification reactants fire retardants and fillers for plastics and silicon rubber composites, coating materials and any of their precursor phases [5-10]. High temperature calcined aluminas are used as ceramic oxides porous ceramics, and

[1] Faculty of Applied Chemistry and Materials Science, University POLITEHNICA of Bucharest, Romania
[2] "ALUM Tulcea" SA, Tulcea, Romania
*Corresponding author e-mail: r_isopescu@chim.upb.ro

castable ceramics [11-14]. Also, both the low and high temperature calcined aluminas serve as raw materials for catalysts and catalyst supports [15-17]. The papers [18-20] offer some more information about properties of these materials. During the thermal treatments, gibbsite undergoes various successive transitions, turning out combinations of various compounds, the most common being the mixtures of boehmite and one or more transitional alumina phases (including χ, κ, γ, δ, θ, η, etc.), more or less amorphous [21]. Always, starting with low temperature gibbsite phase, all the transition phases are arranged on two lines of products, depending on initial pre-treatments applied to the raw materials:

Line 1: Gibbsite → χ-Chi → κ-Kappa → α- Alfa
Line 2: Gibbsite → Boehmite → γ-Gamma → δ-Delta → θ-Teta → α-Alfa.

Moreover, each of the alumina hydrated or anhydrous phases can be a precursor for one special group of transitional or crystalline phases. But most of the research fundamentally aligns to the above concept of two-line transitions, with the gibbsite and boehmite as main precursors for any of the rest of phases [22]. An important aspect of the gibbsite dehydroxilation process is that all the literature reports are indicating clearly the order in which the compounds are formed during the thermal transformations, but did not offer enough data about the kinetics and associated mechanisms of the dehydroxilation processes [23].There are three dynamic factors which control all the transition mechanism from Al_2O_3-$3H_2O$ to α- Al_2O_3: temperature and rate of heating [21-31], particles size dimension of Al_2O_3-$3H_2O$, before the heating treatments [32-35], advanced grinding [36-38] and intensive mechanical activation Al_2O_3-$3H_2O$ raw material [39-42]. In the conditions of special processing of the gibbsite or boehmite, before or during the thermal treatments, paths of transformation (lines 1 and 2) may be modified, and a transitional phase may be added or excluded from the above-mentioned paths of transitions [30, 43, 44]. The kinetic and mechanism of gibbsite phase transitions have been studied with both isothermal and non-isothermal models. These techniques offer important information about the thermal activity of gibbsite or any other phase from the well-known two routes from gibbsite to α-alumina. As example, Radaoui et al, [45] have chosen three of such models, Ozawa-Flynn-Wall (OFW) [46], Akahira-Sunose [47] and Boswell [48] to describe the mechanism and kinetics of gibbsite phase transitions on the line Boehmite → χ-Al_2O_3 → γ-Al_2O_3 → α-Al_2O_3. Based on classical Avrami model [49-51] and of further added reviewed contributors [29, 52, 53], our previous papers demonstrated that all these models are of great importance in TG/DSC data processing [54-59].

The main purpose of the present study is to investigate the alumina gibbsite phase transitions, that occur mainly in the range of 100-400°C, under particularly conditions, where this phase is expected to transform into boehmite

and γ-alumina, and more prevalent into amorphous Al_2O_3 phases with variable water content. Particularly, the investigation aims to highlight the role of particle size dimension as dynamic factor in the mechanism and kinetics of gibbsite transitions to AlO(OH) and γ-Al_2O_3. It has been demonstrated that the thermal decomposition of aluminum hydroxide (gibbsite) follows a specific transitions row with partial recrystallized phases, and substantially depends on both heat treatment and particle size dimension. The Avrami semiempirical model, adapted for non-isothermal transformation [60] was used for kinetic modeling.

2. Materials and Methods

2.1. Sample Preparation.

Aluminum hydroxide sample were received from SC ALUM SA. These samples were produced by Bayer's process and further processed in the newly built line for the production of special grades of dried, milled, and classified aluminium hydroxide, that was recently presented by Dobra et al. [61]. The samples did come from the classified aluminium hydroxide after milling and were dried at 60°C for 3 hours (Table 1). Selection of the sample for mechanism and kinetics investigation is fully described in the papers [18, 19].

Table 1

Samples characteristics

Samples	Granulation	Mineralogy
Sample 1	0 - 150 μm	Al_2O_3-3.H_2O
Sample 2	0 - 4 5 μm	Al_2O_3-3.H_2O
Sample 3	0 - 20 μm	Al_2O_3-3.H_2O
Sample 4	0 - 10 μm	Al_2O_3-3.H_2O
Sample 5	45 – 150 μm	Al_2O_3-3.H_2O

2.2. Characterization Methods

The kinetics parameters of the thermal phase transformations studied in this paper were measured by recording the weight losses and thermal effects occurring during the various dehydration processes on a STA 449 F3 Jupiter device (NETZSCH-Gerätebau GmbH,Selb, Germany). The mineral phases analysis studies by X-ray diffraction (XRD) were carried out using a PANa-lytical Empyrean diffractometer (Almelo, Netherlands). Particle size distributions in the analyzed samples were determined using a Malvern Panalytical Mastersizer 2000 diffraction analyzer (Almelo, The Netherlands). All details about the characterization methods were provided in the papers [18, 19].

3. Kinetic modelling

Solid phase transformations during the dehydroxilation of gibbsite, including recrystallization of new phases and amorphization, were assumed to proceed by a primary nucleation process, followed by nuclei growth. As the heat

flux generated is quite important, the process may be considered as a succession of isothermal transformations that may be modelled by the pseudo-empirical Avrami model [51]. The physical mechanism which is assumed in this model is based on an athermal nucleation mechanism, i.e. the nucleation is instant, while the entire recrystallization process is reduced to a temperature dependent nuclei growth. In isothermal transformation, an Avrami type equation can generally give the relation between the extent of the new phase formation in time, c(t), as:

$$c(t) = 1 - \exp\left[-Kt^n\right] \tag{1}$$

In equation (1) the rate constant K is a measure of the growth rate, and the kinetic exponent *n* is related to the growth mechanism and geometry. Initially, n was considered to have integer values up to 4, a value of 3 or 4 reflecting a volume growth, while lower values (n=1 or n=2) a planar or linear growth

For non-isothermal transformations, the general equation (1) was adapted [60], considering the overall thermal transformation a succession of isothermal processes, where temperature varies as a function of time, T(t). The corresponding extent of the new phase can be calculated as:

$$c(t) = 1 - \exp\left\{-\left[\int_0^t K(T(t))dt\right]^n\right\} \tag{2}$$

The term K(T(t)]) is the kinetic constant of an isothermal process that occurs at temperature T(t) and can be calculated using an Arrhenius type relation:

$$K\left[T(t)\right] = k_0 \exp\left[-E/RT(t)\right] \tag{3}$$

Thus, the equation (2) can then be written:

$$c(t) = 1 - \exp\left\{-\left[\int_0^t k_0 \exp\left(-E/RT(t)\right)dt\right]^n\right\} \tag{4}$$

And the integration may be solved numerically for $0<t<t_f$.

4. Results and Discussion

4.1 Experimental results

Five different gibbsite samples (Table 1), differing by their particle size ranges, were analyzed by TG and DSC at a heating rate of 5°C/min up to 1000ºC (Fig. 1). The mass loss was attributed to the dehydroxilation of gibbsite that led to the successive formation of partially dehydroxilated aluminum oxides and eventually resulting in anhydrous Al_2O_3.

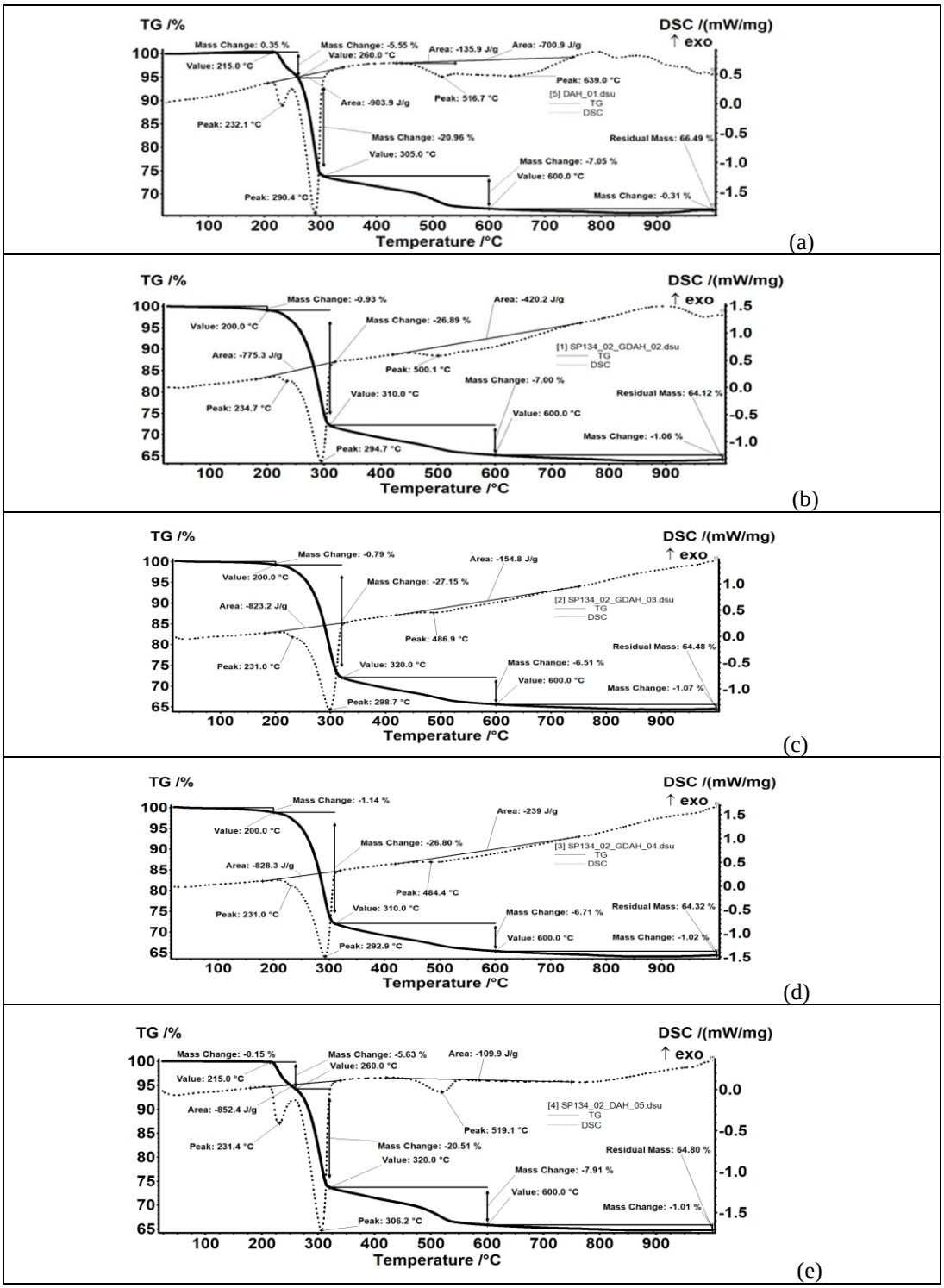

Fig. 1. DSC curves: (a) Sample 1, (b) Sample 2, (c) Sample 3, (d) Sample 4, (e) Sample 5

The thermal effects accompanying the mass loss sustain a four stages transformation. The approximative temperature intervals for these stages are: Stage 1 between 100°C and 200°C, Stage 2 between 200°C and about 320°C, Stage 3 between 425°C and 600°C, and Stage 4 which begins at 600 °C and ends up to 1000°C. The different shapes of DSC curves, mainly for Stage 2, may sustain specific transformations depending on the granulation of the samples. The experimental TG and DSC curves are presented in Fig. 1(a, b, c, d. e.). Analyzing the TG and DSC records, it can be noticed, that in all five samples the overall mass loss (about 35.5%) corresponds to an overall mass balance that characterizes the global reaction of gibbsite dihydroxylation to Al_2O_3. Taking into consideration this mass loss in each sample mentioned above, a small weight loss, about 1% over the temperature range from 100°C to 200°C can be attributed to the loss of adsorbed or sequestrated water in the closed pores. The second step, attributed to the temperature as dynamic factor, ranging from about 200°C to 320°C, has also a particular feature. While the mass loss is about 26% and can be attributed the gibbsite dihydroxylation up to a global formula of $Al_2O_3 \cdot (0.64 \div 0.66)H_2O$, which may be assigned to a partially dehydrated boehmite and/or to partial dehydrated alumina. From the point of view of DSC curve, these processes show specific pathways for each of the five samples as effect of dynamic factor particle size dimension. Samples 1 and sample 5, corresponding to large particles, show a clear two-step transformation, with a first peak at around 232°C (mass loss of 5.5-5.6%) and a second peak at 305-306°C and mass loss of about 20.5%. The samples 3 and sample 4, corresponding to small and very small particles, show a single step transformation with a peak at 298.7°C and 292.9°C. The DSC curve for sample 2 (particles below 45 μm), has an almost imperceptible peak at 234.7°C and a clear peak at 294.7°C, similar to the curves registered for samples 3 and 4. Starting from these observations, two parallel pathways may be assigned to the thermal decomposition of gibbsite in the second step. Consequently, two different emerging solid phases are expected, especially in samples 1 and 5. In order to validate this hypothesis, the solid phases obtained at 260°C, 300°C and 400°C were analyzed by XRD and composition was calculated using Rietveld method. The data, collected from papers [18, 19] are presented in Table 2.

Table 2

Composition of solid phases during thermal decomposition of gibbsite

Sample no.	Particle sizes, μm	Temperature, °C	Composition %			
			Gibbsite	Boehmite	γ-alumina	Amorphous phase
1	0-150	25	41.65	0.00	0.00	58.35
		260	33.30	8.96	0.00	57.74
		300	22.17	10.97	5.90	60.96
		400	2.29	13.59	16.39	67.73

2	0-45	25	62.54	0.00	0.00	37.46
		260	46.42	4.15	0.00	49.43
		300	34.60	5.82	0.57	59.00
		400	3.32	7.45	10.61	78.60
3	0-20	25	61.67	0.00	0.00	38.33
		260	45.41	2.80	0.00	51.79
		300	38.33	4.99	0.44	56.25
		400	0.05	5.44	12.81	81.70
4	0-10	25	62.59	0.00	0.00	37.41
		260	53.23	2.62	0.00	44.15
		300	43.26	5.48	0.64	50.62
		400	2.28	6.86	12.98	77.88
5	45-150	25	55.56	0.00	0.00	44.44
		260	43.48	8.28	0.00	48.24
		300	33.81	11.94	0.00	54.25
		400	0.05	12.86	13.79	73.32

4.2 Kinetic Modelling

For the two possible mechanisms an Avrami type model can be assumed, and kinetic parameters may be estimated by correlation of experimental data. In order to include the two distinct pathways into the model, a new parameter, ω was introduced standing for the initial phase changed fraction according to mechanism 1 and (1- ω) for the fraction that emerged by mechanism 2. DSC curves (fig.1a-e) were integrated over the endothermal transition interval corresponding to step 2. Recrystallized fraction at moment t, in any stage of the process is evaluated by the relation:

$$c(t) = \int_0^t \Delta H(t) \cdot dt \Big/ \int_0^{t_{max}} \Delta H(t) dt \tag{5}$$

where *t* is the time (in seconds) elapsed from the beginning of the transition, computed for a heating rate of 5 °C/minute, and ΔH(t) is the momentary value of energy (W/g) read from the DSC diagram. During data processing, the denominator in relation (5) was checked to give the same value as the thermal effect registered by DSC analysis, in order to ensure a correct interpretation of physical results. The generalization of relation (4) for two mechanisms of phase transformation is given by relations (6-8):

$$c(t) = \omega\left[1 - \exp\left\{-\left[\int_0^t K_1(u)du\right]^{n_1}\right\}\right] + (1-\omega)\left[1 - \exp\left\{-\left[\int_0^t K_2(u)du\right]^{n_2}\right\}\right] \tag{6}$$

$$K_1(u) = \left\{k_{01} \exp\left[-E_1 / RT(u)\right]\right\}^{1/n_1} \tag{7}$$

$$K_2(u) = \left\{k_{02} \exp\left[-E_2 / RT(u)\right]\right\}^{1/n_2} \tag{8}$$

where the kinetic exponents 1 and 2 are assigned to the mechanism 1 and 2, and $K_1(u)$ and $K_2(u)$ are the rate constants for the two mechanisms.
The above model is characterized by seven parameters (n_1, k_{01}, E_1, n_2, E_2, k_{02} and ω), which are to be identified by the minimization of the objective function in form of the least squares:

$$F = \sum_{i=1}^{m} \left[c(t)_{\exp_i} - c(t)_i \right]^2 \quad (9)$$

In relation (9), $c(t)_{exp}$ is the converted volume fraction computed from experimental data, according to equation (5), c(t) is the fraction computed from equation (6), and m is the number of experimental points chosen on the DSC curves. The mathematical model was implemented in Matlab^{TM}(Natick, Ma, USA) release 15, and the minimization was performed using the built-in function *ga* based on genetic algorithms. As the number of model parameters to be identified is high, the genetic algorithm main characteristic, the population size, was established at a value of 500. The low and upper limits for the seven parameters were chosen according to some literature data and general assumptions considered. For the activation energy the search limits were chosen between 100-1000 kJ/mol [31], while for the Avrami kinetic exponents, n_1 and n_2, the search interval was between 1 and 3 to stand for any type of growth mechanism. The goodness of fit by the proposed model was appreciated by the coefficient of determination, R^2 which gives the correlation between experimental and computed values of converted volume. The results obtained are presented in Table 3. For samples 1 and 5, where large particles are present, mechanism 1 may be attributed to the formation of a metastable phase characterized by a linear growth ($1<n_1<2$), caused by a deep perturbation created by heating upon the gibbsite crystalline structure. The perturbation is significant (ω=12-17%) and may stand for metastable ρ-alumina formation that is mentioned also in some other studies [36]. The present Avrami model results give an argument to sustain the formation of ρ-alumina in the thermal treatment of gibbsite. For the samples containing small particles (samples 3 and 4) the contribution of metastable phase formation is not significant. In sample 4, ω=0.02, while the kinetic parameters obtained for sample 3 prove that both transformations are of the same type.

Table 3

Kinetic parameters

Sample no	Particle's size, μm	$k_{0.1}$, s^{-1}	E_1, kJ/mol	n_1	ω	$k_{0,2}$	E_2 kJ/mol	n_2	R^2
1	0-150	7.140e4	78.120	1.42	0.12	7.401e5	143.72	2.77	0.997
2	0-45	9.795e5	92.762	1.86	0.04	5.587e4	119.32	2.39	0.995
3	0-20	4.005e5	109.10	2.17	0.07	3.902e5	128.45	2.33	0.997
4	0-10	7.769e5	77.661	1.15	0.02	7.570e4	118.25	2.31	0.996
5	45-150	6.142e4	84.279	1.65	0.17	7.543e4	131.90	2.67	0.997

The kinetic exponents n_1 and n_2 for sample 3 are greater than 2, standing for a planar growth. Similar observations can also be considered for sample 2. When the particle sizes are small the metastable phase has no time to form, as the rate of phase transformations are high. The two possible distinct mechanism of phase transformations, highlighted by the kinetic modeling, are also evidenced by the temperature dependent evolution of the solid phase presented in Table 2. The samples 3 and 4, with small size particles have a constant increase of amorphous phases in the range of temperatures up to 300°C showing a continuous phase change. In samples 1 and 5, containing large particles, the amorphous phase content varies slightly up to 300°C, while boehmite and γ-alumina are formed, proving that the process takes some two parallel pathways.

5. Conclusions

The kinetic modelling revealed the different pathways of thermal decomposition of the aluminum hydroxide. These pathways are significantly influenced by the particle size range. Small particles evolve by a greater rate and intermediate metastable solid phases have not the time to crystallize. The differences pointed out by the Avrami type model used are in good agreement with measured data concerning the variation with temperature of the solid phase composition.

Acknowledgments:

This study was made possible by the implementation of the "Endow the Research and Development Department of SC ALUM SA Tulcea with independent and efficient research facilities to support the economic competitiveness and business development" project, which was co-funded by the European Regional Development Fund through the Competitiveness Operational Program of 2014–2020. Under this project, the following were purchased and commissioned: "Independent equipment/installation for research and development of the technology for wet aluminum hydroxide classification", equipment/installation for research and development of technology for obtaining the dried aluminum hydroxide", and "Independent equipment/installation for research and development of the technology for grinding and screening the dried aluminum hydroxide"

R E F E R E N C E S

[1]. *H. I. Kim, S. K. Lee*, "Probing the transformation paths from aluminum (oxy)hydroxides (boehmite, bayerite, and gibbsite) to metastable alumina: A view from high-resolution 27Al MAS NMR", Am. Miner., **vol. 106**, 2021, pp. 389–403

[2]. *L. Kovarik, M. Bowden, A. Andersen, N. R. Jaegers, N. Washton, J. Szanyi*, "Quantification of High Temperature Transition Al_2O_3 and Their Phase Transformations", Angew. Chem., **vol. 59**, 2020, pp. 21719–21727

[3]. *H. T. Vo, J. Kim, N. Y Kim, J. K. Lee, J. B. Joo*, "Effect of pore texture property of mesoporous alumina on adsorption performance of ammonia gas", J. Ind. Eng. Chem., **vol. 91**, 2020, pp .129–138

[4]. *L. Wang, C. Shi, L. Wang, L. Pan, X. Zhang, J. Zou, "*Rational design, synthesis, adsorption principles and applications of metaloxide adsorbents: A review", Nanoscale, **vol. 12**, 2020, pp. 4790–4815

[5]. *E. Szatyłowicz, I. Skoczko*, "The use of activated alumina and magnetic field for the removal heavy metals from water", J. Ecol. Eng., **vol. 19**, 2018, pp. 61–67.

[6]. *H. K. Hami, R. F. Abbas, E. M. Eltayef, N. I. Mahdi,* "Applications of aluminum oxide and nano aluminum oxide as adsorbents: Review", Samarra J. Pure Appl. Sci., **vol. 2**, 2020, pp. 19–32.

[7]. *G. D. Vahidi, S. Bajwa, J. Shojaeiarani, N. Stark, A. Darabi*, "Advancements in traditional and nanosized flame retardants for polymers - A review", J. Appl. Polym. Sci., **vol. 138**, 2021, pp. 1-14

[8]. J. Zheng, S. He, J. Wang, W. Fang, Y. Xue, L. Xie, J. Lin, "Performance of Silicone Rubber Composites Filled with Aluminum Nitride and Alumina Tri-Hydrate", Materials, **vol. 13**, 2020, pp. 2489

[9]. *J. Liu Y. Ma, W. Liu, X. Song, S. Yao, J. Wang, M. Cheng, C. Li*, "Preparation of alumina precursor sols with a high solid content for alumina fibers", Materials Research Express, **vol. 6**, 2019, pp. 5207

[10]. *Z. Huim, Y. Baowei, Y. Shuai, H. Jinbao, C. Jixing, L. Wei, S. Yuanyuan, Z. Haiping, Z. Jingxu*, "Research Status and Development of Functional Powder Coating", Chemcial Industry and Engineering. Hydrol. Curr. Res., **vol. 37**, 2020, pp.1–18

[11]. *A. M. Abyzov*, "Aluminum Oxide and Alumina Ceramics (review). Part 1. Properties of Al_2O_3 and Commercial Production of Dispersed Al_2O_3", Refract. Ind. Ceram., **vol. 60**, 2019, pp. 24–32

[12]. *A. M. Abyzov*, "Aluminum Oxide and Alumina Ceramics (Review). Part 2. Foreign Manufacturers of Alumina Ceramics. Technologies and Research in the Field of Alumina Ceramics 1", Refract. Ind. Ceram. **vol. 60**, 2019, pp. 33–42,

[13]. *M. Abyzov*, "Oxide and Alumina Ceramics (Review). Part 3. Russian Manufacturers of Alumina Ceramics", Refract. Ind. Ceram., **vol. 60**, 2019, pp. 183–191,

[14]. *Y. Chen, N. Wang, O. Ola, Y. Xia, Y. Zhu*, "Porous ceramics: Light in weight but heavy in energy and environment technologies", Materials Science and Engineering: R: Reports, **vol.143**, 2021, 100589

[15]. *G. Busca*, "Silica-alumina catalytic materials: A critical review", Catal. Today, **vol. 357**, 2019, pp. 621–629,

[16]. *V.Y. Tregubenko, A.S. Belyi*, "Characterization of Acid-Modified Alumina as a Support for Reforming Catalysts", Kinet. Catal., **vol. 61**, 2020, pp.130–136

[17]. *K. Nikoofar, Y. Shahedi, F.J. Chenarboo*, "Nano Alumina Catalytic Applications in Organic Transformations", Mini-Rev. Org. Chem., **vol. 16**, 2019, pp. 102–110

[18]. *B. S. Vasile, G. Dobra, S. Iliev, L. Cotet, I. A. Neacsu, A. I. Nicoara, V. A. Surdu, A. Boiangiu and L. Filipescu*, "Thermally Activated $Al(OH)_3$: Part I. Morphology and Porosity Evaluation", Ceramics , **vol. 4**, 2021, pp. 265–277

[19]. *B. S. Vasile, G. Dobra, S. Iliev, L. Cotet, I. A. Neacsu, V. A. Surdu, A. I. Nicoara, A. Boiangiu and L. Filipescu*, "Thermally Activated $Al(OH)_3$ Part II—Effect of Different Thermal Treatments", Ceramics, **vol .4**, 2021, pp. 564–575.

[20]. *G. Dobra, B. S. Vasile, S. Iliev, L.Cotet, A. Boiangiu, I. A. Neacsu, A. I. Nicoara, V. A. Surdu, L. Filipescu*, "Technical properties and uses of the aluminum hydroxide, dried, milled and classified" (under press)

[21]. *J.F Brown, D Clark, W.W. Elliott*, "The thermal decomposition of the alumina trihydrate, gibbsite", J. Chem. Soc., 1953, pp 84-88

[22]. *K. Wefers, C. Misra*, "Oxides and Hydroxides of Aluminum", Alcoa Technical Papers no. 18, Revised, 1987

[23]. *P. Nortier, P. Fourre, A.M. Saad, O. Saur, J.C. Lavalley, "*Effects of crystallinity and morphology on the surface properties of alumin", Appl. Catal., **vol 61**, 1990, pp. 141–160.

[24]. *S. Mehta, A. Kalsotra, M. Murat*, "A new approach to phase transformations in gibbsite: The role of the crystallinity", Thermochim. Acta, **vol. 205**, 1992, pp.191–203

[25] *V.I. Lopushan, G.F. Kuznetsov, R.N. Pletnev, D.G. Kleshev*, "Kinetics of phase transitions of gibbsite during heat treatment in air and in water vapor", Refract. Ind. Ceram., **vol. 48**, 2007, pp. 378–382.

[26]. *A.C Vieira Coelho, H.D. Souza Santos, P.K. Kiyohara, K.N.P. Marcos, P.D. Souza Santos*, "Surface Area, crystal morphology and characterization of transition alumina powders from a new gibbsite precursor", Mater. Res., **vol. 10**, 2007, pp. 183–189

[27]. *S.R. Egorova, A.A. Lamberov*, "Effect of the phase composition of gibbsite on the specific surface area of coarse floccule of products formed in its dehydration under thermal treatmen", Russ. J. Appl. Chem., **vol. 87,** 2014, pp. 1021–1030

[28]. *V.V. Danilevich, O. Klimov, K. A. Nadeina, E.Y. Gerasimov, S.V. Cherepanova, Y.V. Vatutina, A.S. Noskov*, "Novel eco-friendly method for preparation of mesoporous alumina from the product of rapid thermal treatment of gibbsite", Superlattices microstruct, **vol.120**, 2018, pp. 148–160

[29]. *H. Van Gog*, "First-principles study of dehydration interfaces between diaspore and corundum, gibbsite and boehmite, and boehmite and γ-Al_2O_3: Energetic stability, interface charge effects, and dehydration defects", Appl. Surf. Sci., **vol. 541**, 2021, pp. 148501

[30]. *I. Ibrahim, S. Baharuddin, R. Arbain, A. Othman, C. Joannes, "*Processing of local bauxite to obtain highly purified and fine alumina powder", in International Conference of Sustainable Earth Resources Engineering 2020 IOP Conference Series: Earth and Environmental Science 641; IOP Publishing:Bristol, UK, 2021.

[31]. *H. Wang, B. Xu, P. Smith, M. Davies, L. DeSilva, C. Wingate*, "Kinetic modelling of gibbsite dehydration/amorphization in the temperature range 823–923 K", Journal of Physics and Chemistry of Solids, **vol. 67**, 2006, pp. 2567–2582

[32]. *B.K. Gan, I.C. Madsenb, J.G. Hockridge*, "In situ X-ray diffraction of the transformation of gibbsite to a-alumina through calcination: Effect of particle size and heating rate", J. Appl. Cryst. **vol. 42**, 2009, pp. 697–705.

[33]. *V.Z. Baranyai, F. Kristály*, "Influence of grain and crystallite size on the gibbsite to boehmite thermal transformation", Studia UBB Chem., **vol. 9**, 2015, pp. 27–44

[34]. *Q. Wang, Y. Li, S. Li, R. Chen, R. Xiang, N. Xu*, "Effects of particle size of $Al(OH)_3$ on the properties of porous purging materials", J. Ceram. Soc. Jpn., **vol. 125**, 2017, pp. 504–508,

[35]. *M. N. Ahmadabadi, A. Nemati, K. Arzani, and S. Baghshahi*, "The relation between particle size and transformation temperature of gibbsite to α-alumina," Miner. Process. Extr. Metall. Trans. Inst. Min. Metall., 2020

[36]. *V.Z. Baranyai, F. Kristály, I. Szűcs*, "Influence of the short time grinding on the thermal decomposition processes of gibbsite produced by the Bayer process", Materials Science and Engineering, **vol.38**, 2013, pp. 15–27

[37]. *J. Kano, S. Saeki, F. Saito, M. Tanjo, S. Yamazaki*, "Application of dry grinding to reduction in transformation temperature of aluminum hydroxides", Int. J. Miner. Process., **vol. 60**, 2000, pp. 91–100,

[38]. *J.R. Mercury, J. Sucupira, M.A. Rodríguez, A. Cabral, A.H. de Aza, P. Pena*, "Influence of the milling conditions on the thermal decomposition of Bayer gibbsite", Powder Technol., **vol. 362**, 2020, pp. 188–196,

[39]. *S.W. Jang, H.Y. Lee, S.M. Lee*, "Mechanical activation effect on the transition of gibbsite to α-alumina", Journal of Materials Science Letters, **vol. 19**, 2000, pp. 507 – 510

[40]. *T. Tsuchida, N. Ichikawa*, "Mechano-chemical phenomena of gibbsite, bayerite and boehmite by grinding", React. Solids, **vol. 7**, 1989, pp. 207–217

[41]. *T. C. Alex, R. Kumar, S. K. Roy, and S. P. Mehrotra*, "Mechanically induced reactivity of gibbsite: Part 1. Planetary milling," Powder Technol., **vol. 264**, 2014, pp. 105-113
[42]. *T. C. Alex, R, Kumar, S. K. Roy, S. P. Mehrotra* "Mechanically induced reactivity of gibbsite: Part 2. Attrition milling", Powder technology, **vol. 264**, 2014, pp. 229-235
[43]. *I. Padilla, S. López-Andrés, A. López-Delgado*, "Effects of Different Raw Materials in the Synthesis of Boehmite and γ- and α-Alumina", J. Chem., 2016, pp. 5353490
[44]. *R.W.N.D. Filho, G.D.A. Rocha, C.R. Montes, A.C. Vieira-Coelho*, "Synthesis and Characterization of Boehmites Obtained from Gibbsite in Presence of Different Environments", Mater. Res., **vol. 19**, 2016, pp. 659–668
[45]. *D. Redaoui, F. Sahnoune, M. Heraiz and A. Raghdi*, "Mechanism and Kinetic Parameters of the Thermal Decomposition of Gibbsite Al(OH)3 by Thermogravimetric Analysis",, Acta Physica Polonica A, **vol. 132**, no. 3, 2017, pp. 562-565
[46]. *T. Ozawa*, "A new method of analyzing thermogravimetric data", Bulletin of the Chemical Society of Japan, **vol. 38**, 1965, pp. 1881-1886
[47]. T, *Akahira, T. Sunose*, "Method of determining activation deterioration constant of electrical insulating materials", Research Report, Chiba Institute Technology, **vol. 16**, 1971, pp.22–31
[48.] *P.G. Boswell*, "On the calculation of activation energies using a modified Kissinger method", Journal of Thermal Analysis and Calorimetry, **vol. 18**, 1980, pp. 353–358
[49]. *M. Avrami*, "Kinetics of Phase Change. I. General Theory", J. Chem. Phys., vol 7, 1939, pp. 1103 - 1112
[50]. *M. Avrami*, "Kinetics of Phase Change. II. Transformation-Time Relations for Random Distribution of Nuclei", J. Chem. Phys, **vol. 8,** 1940, pp. 212-225
[51]. *M. Avrami*, "Kinetics of phase change. III. Granulation, phase change and microstructure", J Chem Phys, **vol. 9**,1941, pp. 177–184
[52]. *A.C. Faleirosa , T.N. Rabeloa , G.P. Thimb, M.A.S. Oliveira*, "Kinetics of Phase Change", Materials Research, **vol. 3**, 2000, pp. 51-60
[53]. *E. Piorkowskaa, A. Galeskia, J. M. Haudin*, "Critical assessment of overall crystallization kinetics theories and predictions", Prog. Polym. Sci. vol. 31, 2006, pp. 549–57
[54]. *A. Woinarosky, R. Isopescu, S. Şerban*, "Identification of solid phases in mixtures of crystallized sodium silicates", Proceedings of 5th World Congress on Chemical Engineering, San Diego, 1996, **vol. 4**, 685-692
[55.] *L. Filipescu, R. Isopescu, M. Mocioi, F. Zahanagiu*, "Mechanisms and kinetics of sodium disilicate crystallization", 14th Int. Symp. on Ind. Crystalization, Cambridge, UK, 1999, Paper 122
[56]. *A. Woinaroschy, R. Isopescu, L. Filipescu*, "X-Ray Patterns Identification of Crystallized Sodium Disilicates Mixtures" Cryst. Res. Technol., **vol. 35**, 2000, pp. 969–977
[57]. *R. Isopescu, M. Mocioi, F. Zahanagiu, L. Filipescu*, "Mechanism and kinetics of the sodium disilicate crystallisation", Rev. Chimie, **vol.50,** no. 8, 1999, pp.579-584
[58.] *R. Isopescu, M. Calogrea, M. E. Cîrjaliu-Murgea, L. Filipescu*, "Stabilized Ammonium nitrate", The 35th National conference on chemistry, Romanian Academy, RM. Valcea, 2004
[59]. *R. Isopescu, S. Serban, C. Radovici, L. Filipescu*, "Thermal analysis of binary and ternary systems ammonium nitrate, ammonium sulphate and ammonium dihydrogen orthophosphate", 13th Romanian International Conferince on Chemistry and Chemical Engineering, 2005
[60]. *K. Nakamura, T. Watanabe, K. Katayama, T. Amano*," Some aspects of nonisothermal crystallization of polymers. I. Relationship between crystallization temperature, crystallinity, and cooling conditions". Journal of Applied Polymer Science, **vol.16**, no. 5, 1972, pp.1077–1091.
[61]. *G. Dobra, S, Garcia-Granda, S. Iliev, L. Cotet, I. Hulka, P. Negrea, N. Duteanu, A. Boiangiu, L. Filipescu*, "Aluminum hydroxide impurities occlusions and contamination Sources", Rev. Chim., **vol 71**, 2020, pp. 65–76.